

Multi-Objective Policy Generation for Multi-Robot Systems Using Riemannian Motion Policies

Anqi Li, Mustafa Mukadam, Magnus Egerstedt and Byron Boots

Institute for Robotics and Intelligent Machines

Georgia Institute of Technology

Atlanta, Georgia 30332

Email: {anqi.li, mhmukadam, magnus}@gatech.edu,
bboots@cc.gatech.edu

Abstract—In the multi-robot systems literature, control policies are typically obtained through descent rules for a potential function which encodes a single team-level objective. However, for multi-objective tasks, it can be hard to design a single control policy that fulfills all the objectives. In this paper, we exploit the idea of decomposing the multi-objective task into a set of simple subtasks. We associate each subtask with a potentially lower-dimensional manifold, and design Riemannian Motion Policies (RMPs) on these manifolds. Centralized and decentralized algorithms are proposed to combine these policies into a final control policy on the configuration space that the robots can execute. We propose a collection of RMPs for simple multi-robot tasks that can be used for building controllers for more complicated tasks. In particular, we prove that many existing multi-robot controllers can be closely approximated by combining the proposed RMPs. Theoretical analysis shows that the multi-robot system under the generated control policy is stable. The proposed framework is validated through both simulated tasks and robotic implementations.

I. INTRODUCTION

Multi-robot coordination strategies are typically designed to achieve *single* team-level objectives with provable guarantees, e.g. forming a certain shape, covering an area of interest, or meeting at a common location [7, 16]. However, practical problems often involve a diverse set of objectives. For example, collision avoidance and connectivity maintenance are often required in addition to the primary tasks [22]. One possible solution is to encode the multi-objective problem as a single motion planning problem with various constraints [11, 21, 14, 20]. However, the more objectives considered, the more difficult it is to directly search for a solution that can achieve *all* of the objectives simultaneously.

An alternative strategy is to design controllers for each individual objective and then *combine* them into a single controller. Different schemes for combining controllers have been investigated extensively in the multi-robot systems literature. For example, one standard treatment for collision avoidance is to let the collision avoidance controller take over the operation if there is a risk of collision [4]. Another example is the potential field method, which formulates a global controller as a weighted sum of controllers for each objective [4, 13]. A main challenge for these constructions, however, is that unexpected interaction between individual controllers may lead to undesirable and even catastrophic behaviors – in other words,

the provable properties of the individual controllers can be nullified [1, 5]. Null-space-based behavioral control [3] partially overcomes this problem by assigning priorities to controllers and ensuring that controllers of lower priority only act on the null-space of controllers with higher priority. However, it is specially designed for a particular class of behaviors. Methods based on Control Lyapunov Functions (CLFs) and Control Barrier Functions (CBFs) [1, 22] seek to optimize primary task-level objectives while formulating secondary objectives as CLF or CBF constraints and solve via quadratic programming (QP). However, solving the QP typically requires centralized computation and can be computationally demanding if the number of robots and number of constraints are large.

In this paper, we rethink how an objective and its corresponding controller are defined. Instead of defining objectives on the configuration space (which is often assumed to be Euclidean), we consider objectives defined on *manifolds*, which could be of lower dimension than the configuration space and non-Euclidean. An example of a non-Euclidean objective is obstacle avoidance, where obstacles become holes in the space and the geodesics flow around them [19]. To describe controllers on manifolds, we use the Riemannian Motion Policy (RMP) [19, 8], a manifold-oriented mathematical object that has been successfully used for robot manipulators.

There are three major advantages to defining objectives and controllers on manifolds. First, this formulation provides a powerful new way to reason about controllers designed for different objectives. Rather than defining controllers in configuration space, we design the controller in the space most relevant to its objective. Since the manifolds are usually of lower dimension than the configuration space, this can provide additional degrees of freedom that help controllers avoid conflicts. Second, Riemannian metrics on manifolds naturally provide a geometrically-consistent notion of importance when combining controllers. It is shown in [8] that a combined controller is Lyapunov-stable given that all component controllers are generated from a class of dynamical systems called *Geometric Dynamical Systems* (GDSs). Third, since RMPs are coordinate-free, the framework can be generalized to heterogeneous multi-robot teams.

We present several contributions in this paper. First, we propose a centralized solution to integrate controllers described

by RMPs such that the resulting controller is Lyapunov-stable. Second, we propose a decentralized algorithm that resembles the features of the centralized solution. Third, we draw a direct connection between a large group of existing multi-robot distributed controllers and RMPs and show how RMPs can achieve similar behavior.

The rest of this paper is organized as follows. Section II briefly revisits Riemannian Motion Policies (RMPs) and RMPflow, the algorithm for control policy generation with RMPs. Section III and Section IV discusses centralized and decentralized RMP frameworks for multi-robot systems, respectively. Finally, experimental results and conclusions are presented in Section V and Section VI, respectively.

II. RIEMANNIAN MOTION POLICIES (RMPs)

We briefly review Riemannian Motion Policies (RMPs) [19, 8], a mathematical representation of policies on manifolds, and RMPflow [8], a recursive algorithm to combine RMPs.

Consider a robot (or a group of robots in later sections) with its configuration space \mathcal{C} being a smooth d -dimensional manifold. Without loss of generality, we assume that \mathcal{C} admits a global *generalized coordinate* $\mathbf{q} : \mathcal{C} \rightarrow \mathbb{R}^d$. As is the case in [8], we assume that the system can be feedback linearized in such a way that it is controlled directly through the generalized acceleration, $\ddot{\mathbf{q}} = \pi(\mathbf{q}, \dot{\mathbf{q}})$. We call π a *policy* or a *controller*, and $(\mathbf{q}, \dot{\mathbf{q}})$ the *state*. Oftentimes, the task is defined on a different manifold called the *task space*, denoted \mathcal{T} . Note that the task can be the composition of a set of *subtasks*, for example, avoiding collision with a certain obstacle, reaching a goal, tracking a trajectory, etc. In this case, the task space becomes a collection of multiple *subtask spaces*, each corresponding to a subtask. We assume that the task space \mathcal{T} is related to the configuration space \mathcal{C} through a smooth *task map* $\psi : \mathcal{C} \rightarrow \mathcal{T}$. Then, the goal of this paper is to generate policy π in configuration space \mathcal{C} so that the transformed trajectory exhibits desired behaviors on the task space \mathcal{T} .

A. Riemannian Motion Policies

Riemannian Motion Policies (RMPs) [19] represent policies on manifolds. Consider an m -dimensional manifold \mathcal{M} with a global coordinate $\mathbf{x} \in \mathbb{R}^m$. Assume that $\dot{\mathbf{x}}$ can be directly controlled, i.e. $\mathbf{u} = \dot{\mathbf{x}}$. An RMP on \mathcal{M} can be represented by two forms, its *canonical form* and its *natural form*. The *canonical form* of an RMP is a pair $(\mathbf{u}, \mathbf{M})^{\mathcal{M}}$, where $\mathbf{u} : (\mathbf{x}, \dot{\mathbf{x}}) \mapsto \mathbf{u}(\mathbf{x}, \dot{\mathbf{x}}) \in \mathbb{R}^m$ is the desired acceleration, i.e. control input, and $\mathbf{M} : (\mathbf{x}, \dot{\mathbf{x}}) \mapsto \mathbf{M}(\mathbf{x}, \dot{\mathbf{x}}) \in \mathbb{R}_+^{m \times m}$ is the inertial matrix which defines the importance of the RMP when combined with other RMPs. Given its canonical form, the *natural form* of an RMP is the pair $[\mathbf{f}, \mathbf{M}]^{\mathcal{M}}$, where $\mathbf{f} = \mathbf{M}\mathbf{u}$ is the desired force. The natural forms of RMPs are introduced mainly for computational convenience.

The inertial matrix \mathbf{M} can be considered as an outcome of a Riemannian metrics on the *tangent bundle* of the manifold \mathcal{M} , denoted as $T\mathcal{M}$. Let $\mathbf{G} : (\mathbf{x}, \dot{\mathbf{x}}) \mapsto \mathbf{G}(\mathbf{x}, \dot{\mathbf{x}}) \in \mathbb{R}_+^{m \times m}$

be a Riemannian metric on $T\mathcal{M}$. It introduces the following *curvature terms* on the tangent bundle $T\mathcal{M}$,

$$\begin{aligned}\Xi_{\mathbf{G}}(\mathbf{x}, \dot{\mathbf{x}}) &:= \frac{1}{2} \sum_{i=1}^m \dot{x}_i \partial_{\mathbf{x}} \mathbf{g}_i(\mathbf{x}, \dot{\mathbf{x}}), \\ \xi_{\mathbf{G}}(\mathbf{x}, \dot{\mathbf{x}}) &:= \ddot{\mathbf{G}}(\mathbf{x}, \dot{\mathbf{x}}) \dot{\mathbf{x}} - \frac{1}{2} \nabla_{\mathbf{x}} (\dot{\mathbf{x}}^{\top} \mathbf{G}(\mathbf{x}, \dot{\mathbf{x}}) \dot{\mathbf{x}}),\end{aligned}\quad (1)$$

where $\ddot{\mathbf{G}}(\mathbf{x}, \dot{\mathbf{x}}) := [\partial_{\mathbf{x}} \mathbf{g}_i(\mathbf{x}, \dot{\mathbf{x}}) \dot{\mathbf{x}}]_{i=1}^m$, $\mathbf{g}_i(\mathbf{x}, \dot{\mathbf{x}})$ is the i th column of $\mathbf{G}(\mathbf{x}, \dot{\mathbf{x}})$, and x_i is the i th component of \mathbf{x} . The inertial matrix $\mathbf{M}(\mathbf{x}, \dot{\mathbf{x}})$ is then related to the Riemannian metric $\mathbf{G}(\mathbf{x}, \dot{\mathbf{x}})$ through,

$$\mathbf{M}(\mathbf{x}, \dot{\mathbf{x}}) = (\mathbf{G}(\mathbf{x}, \dot{\mathbf{x}}) + \Xi_{\mathbf{G}}(\mathbf{x}, \dot{\mathbf{x}})). \quad (2)$$

When the metric is not velocity dependent, i.e. $\mathbf{G}(\mathbf{x}, \dot{\mathbf{x}}) = \mathbf{G}(\mathbf{x})$, we have $\Xi_{\mathbf{G}} = \mathbf{0}$ and $\mathbf{M}(\mathbf{x}) = \mathbf{G}(\mathbf{x})$.

RMPs on a manifold \mathcal{M} can be naturally (but not necessarily) generated from a class of systems called *Geometric Dynamical Systems* (GDSs) [8]. The dynamics of GDSs are in the form of

$$\mathbf{M}(\mathbf{x}, \dot{\mathbf{x}}) \ddot{\mathbf{x}} + \xi_{\mathbf{G}}(\mathbf{x}, \dot{\mathbf{x}}) = -\nabla_{\mathbf{x}} \Phi(\mathbf{x}) - \mathbf{B}(\mathbf{x}, \dot{\mathbf{x}}) \dot{\mathbf{x}}, \quad (3)$$

where $\mathbf{B} : \mathbb{R}^m \times \mathbb{R}^m \rightarrow \mathbb{R}_+^{m \times m}$ is the *damping matrix*, and $\Phi : \mathbb{R}^m \rightarrow \mathbb{R}$ is the *potential function*. A GDS can be represented by a tuple $(\mathcal{M}, \mathbf{G}, \mathbf{B}, \Phi)$. In the specific case when $\mathbf{G}(\mathbf{x}, \dot{\mathbf{x}}) = \mathbf{G}(\mathbf{x})$, the GDSs reduce to the widely studied *Simple Mechanical Systems* (SMSs) [6]. An RMP $(\mathbf{u}, \mathbf{M})^{\mathcal{M}}$ is naturally associated with the GDS by solving for $\mathbf{u} = \dot{\mathbf{x}}$ from (3) and computing \mathbf{M} through (2).

B. RMPflow

RMPflow is a recursive algorithm to generate control policies on the configuration space given the RMPs for every subtask, for example, collision avoidance with a particular obstacle, reaching a goal, etc. RMPflow introduces: 1) a data structure, called the *RMP-tree*, to describe the tree-structured task map ψ and the policies, and 2) a set of operators, called the *RMP-algebra*, to propagate information across the RMP-tree.

An RMP-tree is a directed tree. Each node v represents a state $(\mathbf{x}, \dot{\mathbf{x}})$ defined over a manifold \mathcal{M} together with an associated RMP $(\mathbf{u}, \mathbf{M})^{\mathcal{M}}$. With a slight abuse of notation, we let $v = ((\mathbf{x}, \dot{\mathbf{x}}), (\mathbf{u}, \mathbf{M})^{\mathcal{M}})$. Each edge e corresponds to a smooth map from the parent node to the child node, denoted as ψ_e . RMPflow assumes that the task space \mathcal{T} is related to the configuration space \mathcal{C} through a tree-structured task map. The root node of the RMP-tree r describes the state of the robot (or a group of robots in the subsequent section) and its control policy on the configuration space, $r = ((\mathbf{q}, \dot{\mathbf{q}}), (\mathbf{u}_r, \mathbf{M}_r)^{\mathcal{C}})$. Each leaf node l represents a subtask with RMP $\{(\mathbf{u}_l, \mathbf{M}_l)^{\mathcal{T}_l}\}$, where \mathcal{T}_l is a subtask space.

To illustrate how the RMP-algebra operates, consider a node p with K child nodes. Let $\{v_j\}_{j=1}^K$ and $\{e_j\}_{j=1}^K$ denote the child nodes and corresponding edges from p to child nodes, respectively. Suppose that p describes a policy on manifold \mathcal{M} with coordinate \mathbf{x} , and v_j describes a policy on manifold

\mathcal{N}_j with coordinate \mathbf{y}_j . We then denote $p = ((\mathbf{x}, \dot{\mathbf{x}}), [\mathbf{f}, \mathbf{M}]^{\mathcal{M}})$ and $v_j = ((\mathbf{y}_j, \dot{\mathbf{y}}_j), [\mathbf{f}_j, \mathbf{M}_j]^{\mathcal{N}_j})$, where $\mathcal{N}_j = \psi_{e_j}(\mathcal{M})$. Note that here we represent the RMPs in their natural form. The RMP-algebra consists of the following three operators:

- 1) **pushforward** is the operator to forward propagate the *state* from the parent node p to its child nodes $\{v_j\}_{j=1}^K$. Given $(\mathbf{x}, \dot{\mathbf{x}})$ from p , it computes $(\mathbf{y}_j, \dot{\mathbf{y}}_j) = (\psi_{e_j}(\mathbf{x}), \mathbf{J}_j(\mathbf{x}) \dot{\mathbf{x}})$ for each child node v_j , where $\mathbf{J}_j = \partial_{\mathbf{x}} \psi_{e_j}$ is the Jacobian matrix.
- 2) **pullback** is the operator to backward propagate the natural-formed RMPs from the child nodes to the parent node. Given $\{[\mathbf{f}_j, \mathbf{M}_j]^{\mathcal{N}_j}\}_{j=1}^K$, the RMP for the parent node p is computed as,

$$\mathbf{f} = \sum_{j=1}^K \mathbf{J}_j^\top (\mathbf{f}_j - \mathbf{M}_j \dot{\mathbf{J}}_j \dot{\mathbf{x}}), \quad \mathbf{M} = \sum_{j=1}^K \mathbf{J}_j^\top \mathbf{M}_j \mathbf{J}_j. \quad (4)$$

It can be shown that the canonical form $(\mathbf{u}, \mathbf{M})^{\mathcal{M}}$ of the above RMP is the solution to the least-squares problem,

$$\mathbf{u} = \arg \min_{\mathbf{u}'} \frac{1}{2} \sum_{j=1}^K \|\mathbf{J}_j \mathbf{u}' + \dot{\mathbf{J}}_j \dot{\mathbf{x}} - \mathbf{u}_j\|_{\mathbf{M}_j}^2 \quad (5)$$

where $\mathbf{u}_j = \mathbf{M}_j^\dagger \mathbf{f}_j$, and $\|\cdot\|_{\mathbf{M}_j}^2 = \langle \cdot, \mathbf{M}_j \cdot \rangle$, \dagger denotes the Moore-Penrose inverse.

- 3) **resolve** maps an RMP from its natural form to its canonical form. Given $[\mathbf{f}, \mathbf{M}]^{\mathcal{M}}$, it outputs $(\mathbf{u}, \mathbf{M})^{\mathcal{M}}$ with $\mathbf{u} = \mathbf{M}^\dagger \mathbf{f}$.

With the RMP-tree specified, RMPflow can perform control policy generation. RMPflow first performs a forward pass: it recursively calls **pushforward** from the root node to the leaf nodes to update the state information in each node in the RMP-tree. Secondly, every leaf node l *evaluates* its natural form RMP $\{(\mathbf{f}_l, \mathbf{M}_l)^{\mathcal{T}_l}\}$ possibly given by its GDS. Then, RMPflow performs a backward pass: it recursively calls **pullback** from the leaf nodes to the root node to back propagate the RMPs in the natural form. Finally, RMPflow calls **resolve** at the root node to transform the RMP $[\mathbf{f}_r, \mathbf{M}_r]^{\mathcal{C}}$ into its canonical form $(\mathbf{u}_r, \mathbf{M}_r)^{\mathcal{C}}$ to solve for the control input.

C. Stability Properties of RMPflow

To establish the stability results, we assume that every leaf node is generated from a GDS. Before stating the stability theorem, we need to define the metric, damping matrix, and potential function for a *node* in the RMP-tree.

Definition II.1. *If a node is a leaf, its metric, damping matrix and potential are defined as it is defined in its underlying GDS. The metric, damping matrix and potential for a non-leaf node with K children is defined recursively through the following relationship,*

$$\mathbf{G} = \sum_{j=1}^K \mathbf{J}_j^\top \mathbf{G}_j \mathbf{J}_j, \quad \mathbf{B} = \sum_{j=1}^K \mathbf{J}_j^\top \mathbf{B}_j \mathbf{J}_j, \quad \Phi = \sum_{j=1}^K \Phi_j \circ \mathbf{y}_j, \quad (6)$$

where G_j , B_j and Φ_j be the metric, damping matrix, and potential for the j th child, respectively.

Note, however, that a non-leaf node generally does *not* follow the GDS given by its corresponding metric, damping matrix, and potential. We refer the readers to [8] for more formal treatments of these concepts. The stability results of RMPflow is stated in the following theorem.

Theorem II.1 (Cheng et al. [8]). *Let \mathbf{G}_r , \mathbf{B}_r , and Φ_r be the metric, damping matrix, and potential function of the root node defined in (6). If $\mathbf{G}_r, \mathbf{B}_r \succ 0$, the system converges to a forward invariant set $\mathcal{C}_\infty := \{(\mathbf{q}, \dot{\mathbf{q}}) : \nabla_{\mathbf{q}} \Phi_r = 0, \dot{\mathbf{q}} = 0\}$.*

III. CENTRALIZED CONTROL POLICY GENERATION FOR MULTI-ROBOT SYSTEMS

We begin by formulating a control policy generation algorithm for multi-robot systems directly based on RMPflow. This algorithm is *centralized* because it requires a centralized processor to collect the states of *all* robots and solve for the control input for *all* robots jointly given *all* the subtasks. In Section IV, we introduce a decentralized algorithm that resembles the features of the centralized algorithm.

Consider a potentially heterogeneous¹ team of N robots indexed by $\mathcal{I} = \{1, \dots, N\}$. Let \mathcal{C}_i be the configuration space of robot i with \mathbf{q}_i being a global coordinate on \mathcal{C}_i . The configuration space is then the product manifold $\mathcal{C} = \mathcal{C}_1 \times \dots \times \mathcal{C}_N$. As in Section II, we assume that each robot is feedback linearized. We model the control policy for each robot as a second-order differential equation $\ddot{\mathbf{q}}_i = \pi_i(\mathbf{q}_i, \dot{\mathbf{q}}_i)$. An obvious example is a team of mobile robots with double integrator dynamics on \mathbb{R}^2 , where the generalized coordinate is the coordinates on that space themselves.

Let \mathcal{L} denote the set of all subtasks, where each subtask $l \in \mathcal{L}$ is specified through an RMP on a manifold \mathcal{T}_l . In particular, in all the examples in this paper, the RMPs are generated by GDSs in the form of (3). Here we assume that the subtasks are *pre-allocated* in the sense that each subtask l is defined for a specified subset of robots \mathcal{I}_l . Examples of subtasks include collision avoidance between a pair of robots (a binary subtask), trajectory following for a robot (a unitary subtask), etc. Let $\psi_j : \prod_{k \in \mathcal{I}_j} \mathcal{C}_k \rightarrow \mathcal{T}_j$ be the transformation from the product configuration space to the task space.

The above formulation gives us an alternative view of multi-robot systems with emphasis on their multi-task nature. Rather than encoding the team-level task as a global potential function (as is commonly done in the multi-robot literature), we decompose the task as *local* subtasks defined for subsets of robots, and design policies for individual subtasks. The main advantage is that as the task becomes more complex, it becomes increasingly difficult to design a single potential function that renders the desired global behavior. However, it is often natural to decompose global tasks into local subtasks, even for complex tasks, since multi-robot tasks can often come from local specifications [16, 9, 7]. Therefore, this formulation provides a relatively straightforward generalization to multi-objective tasks. Moreover, this subtask formulation allows us

¹See Section V-C for a discussion about heterogeneous teams.

to borrow existing controllers designed for single-robot tasks, such as collision avoidance, goal reaching, etc.

Recall from Section II that RMPflow operates the RMP-algebra on an RMP-tree, a tree structure describing the task space. The main objective of this section is to construct an RMP-tree for general multi-robot problems. Note that given a set of subtasks, the construction of the RMP-tree is not unique. One way to construct an RMP-tree is to use non-leaf nodes to represent subset of the team:

- The root node represents the control policy on the configuration space $\mathcal{C} = \mathcal{C}_1 \times \dots \times \mathcal{C}_N$.
- Any leaf l of the RMP-tree is a user-specified policy represented as an RMP on a subtask space manifold \mathcal{T}_l .
- The parent of any leaf RMP l is $\prod_{i \in \mathcal{I}_l} \mathcal{C}_i$, where \mathcal{I}_l are the robots that subtask l is defined on.
- Every non-leaf node represents a control policy on a product space of the configuration space of a set of individual robots.
- Consider two non-leaf nodes v_i and v_j such that v_j is a decedent of v_i in the RMP-tree. Let \mathcal{I}_{v_i} and \mathcal{I}_{v_j} be the subset of robots for node v_i and v_j , respectively. Then $\mathcal{I}_{v_j} \subseteq \mathcal{I}_{v_i}$.

Figure 1 shows an example RMP-tree for a team of three robots. The robots are tasked with forming a certain shape and reaching a goal while avoiding inter-robot collisions. The root of the RMP-tree is defined on the configuration space for the team, which is the Cartesian product of the configuration spaces for all three robots. On the second level, the nodes represent subsets of robots which, in this case, are pairs of robots. Several leaf nodes, such as collision avoidance and distance preservation RMPs are connected to these nodes as they are defined for pairs of robots. One level deeper is the node corresponding to the configuration space for robot 1, the leader robot. The goal attractor RMP is connected to this node since the goal reaching subtask is assigned to the leader only.

Note that branching in the RMP-tree does not necessarily define a partition over robots. Let v_i and v_j be children of the same node p and let \mathcal{I}_{v_i} and \mathcal{I}_{v_j} be the subset of robots for node v_i and v_j , respectively. Then it is *not* necessary that $\mathcal{I}_{v_i} \cap \mathcal{I}_{v_j} = \emptyset$. For example, in Fig. 1, the three nodes on the second level are defined for subsets $\{1, 2\}$, $\{2, 3\}$, and $\{3, 1\}$, respectively. The intersection of any two of them is not empty. In fact, if a branching is indeed a partition, then the problem can be split into *independent* sub-problems. For multi-robot systems, this means that the team consists of independent sub-teams with completely independent tasks. This rarely occurs since common overarching missions, such as collision avoidance, often involves sub-tasks defined for *every* pair of robots.

According to Theorem II.1, it is guaranteed that the controller generated by RMPflow drives the system to a forward invariant set $\mathcal{C}_\infty := \{(\mathbf{q}, \dot{\mathbf{q}}) : \nabla_{\mathbf{q}} \Phi_r = 0, \dot{\mathbf{q}} = 0\}$ if $\mathbf{G}_r, \mathbf{B}_r \succ 0$, where $\mathbf{G}_r, \mathbf{B}_r$ and Φ_r are defined recursively through (6). In other words, this guarantees that the resulting system is stable, which is important: unstable behaviors such as high-frequency oscillation are avoided and stability provides

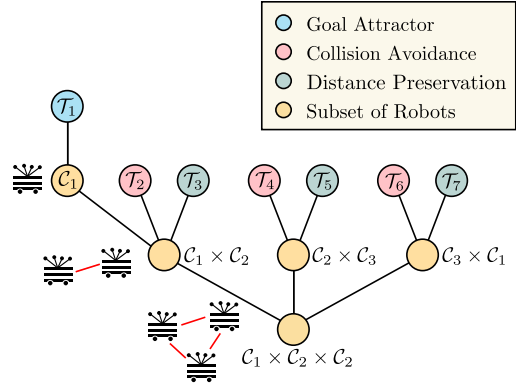


Fig. 1: An example of an RMP-tree for a group of three robots performing a formation preservation task. The root represents the entire team and the second level represents pairs of robots. The subtask RMPs defined for pairs of robots, for example, collision avoidance and distance preservation, are attached to these nodes. The goal attractor RMP is connected to the node representing the configuration space for robot 1, the leader.

formal guarantees on the performance of certain types of subtasks such as collision avoidance².

To elucidate the process of designing RMPs and to connect to relevant multi-robot tasks, we provide examples of RMPs for multi-robot systems that can produce complex behaviors when combined. In the following, we use \mathbf{x}_i to denote the coordinate of robot i in \mathbb{R}^2 . An additional transformation can be composed with the given task maps for robots with other configuration spaces.

A. Pairwise Collision Avoidance

When robots are operating as a team, inter-robot collisions should be avoided. We formulate collision avoidance as ensuring a minimum safety distance D_s for every pair of robots. To generate collision-free motions, for any two robots $i, j \in \mathcal{I}$, we construct an RMP leaf node for the pair. The subtask space is the 1-d distance space, i.e. $\mathbf{x} = \psi(\mathbf{x}_i, \mathbf{x}_j) = \|\mathbf{x}_i - \mathbf{x}_j\|/D_s - 1$.

To ensure a safety distance between the pair, we use a construction similar to the collision avoidance RMP for static obstacles in [8]. The metric for the pairwise collision avoidance RMP is defined as $\mathbf{G}(\mathbf{x}, \dot{\mathbf{x}}) = w(\mathbf{x}) u(\dot{\mathbf{x}})$, where $w(\mathbf{x}) = \frac{1}{\mathbf{x}^4}$, $u(\dot{\mathbf{x}}) = \epsilon + \min(0, \dot{\mathbf{x}}) \dot{\mathbf{x}}$ with a small positive scalar $\epsilon > 0$. The metric retains a large value when the robots are close to each other (\mathbf{x} is small), and when the robots are moving fast towards each other ($\dot{\mathbf{x}} < 0$ and $|\dot{\mathbf{x}}|$ is large). Conversely, the metric decreases rapidly as \mathbf{x} increases. Recall that the metric is closely related to the inertial matrix, which determines the importance of the RMP when combined with other policies. This means that the collision avoidance RMP will dominate when robots are close to each other or moving fast towards each other, while it has almost no effect on the resulting controller when the robots are far from each other.

²See Section III-A

We next design the GDS that generates the collision avoidance RMP. The potential function is defined as $\Phi(\mathbf{x}) = \frac{1}{2}\alpha w(\mathbf{x})^2$ and the damping as $\mathbf{B}(\mathbf{x}, \dot{\mathbf{x}}) = \eta \mathbf{G}(\mathbf{x}, \dot{\mathbf{x}})$, where α, η are positive scalars. As the robots approach the safety distance, the potential function $\Phi(\mathbf{x})$ approaches infinity. Due to the stability guarantee of RMPflow, this barrier-type potential will always ensure that the distance between robots is greater than D_s . Since the inertial matrix also approaches infinity, collision avoidance will dominate other policies, ensuring that the resulting control policy from RMPflow is *always* collision-free.

B. Pairwise Distance Preservation

Another common task for multi-robot systems is to form a specified shape or formation. This can be accomplished by maintaining the inter-robot distance between certain pairs of robots. Therefore, formation control can be induced by an RMP leaf that maintains distances. Such an RMP can be defined on the 1-d distance space, $\mathbf{x} = \psi(\mathbf{x}_i, \mathbf{x}_j) = \|\mathbf{x}_i - \mathbf{x}_j\| - d_{ij}$, where d_{ij} is the desired distance between robot i and robot j . For the GDS, we use a constant metric $\mathbf{G} \equiv c \in \mathbb{R}_{++}$. The potential function is defined as $\Phi(\mathbf{x}) = \frac{1}{2}\alpha \mathbf{x}^2$ and the damping is $\mathbf{B}(\mathbf{x}, \dot{\mathbf{x}}) = \eta$, with $\alpha, \eta > 0$. We will refer to this RMP as a *Distance Preservation RMPa* in later sections.

Note that the above RMP is not equivalent to the potential-based formation controller in, e.g. [16, 9]. However, there does exist an RMP that has very similar behavior. It is defined on the product space, $\mathbf{x} = (\mathbf{x}_i, \mathbf{x}_j)$. The metric for the RMP is also constant, $\mathbf{G} \equiv c \in \mathbb{R}_{++}$. The potential function is defined as $\Phi(\mathbf{x}) = \frac{1}{2}\mathcal{E}_{ij}(\|\mathbf{x}_i - \mathbf{x}_j\|)$, where $\mathcal{E}_{ij} : \mathbb{R} \rightarrow \mathbb{R}$ is differentiable and achieves its minimum at d_{ij} . Common choices include $\mathcal{E}_{ij}(s) = (s - d_{ij})^2$ and $\mathcal{E}_{ij}(s) = (s^2 - d_{ij}^2)^2$ [16]. Damping is defined as $\mathbf{B}(\mathbf{x}, \dot{\mathbf{x}}) = \eta \mathbf{I}$, with $\alpha, \eta > 0$. This RMP will be referred to as *Distance Preservation RMPb* in later sections.

When there are only distance preserving RMPs in the tree. The resulting individual-level dynamics is given by,

$$\ddot{\mathbf{x}}_i = -\frac{\alpha}{c D_i} \sum_{j:(i,j) \in E} \partial_{x_i} \mathcal{E}_{ij}(\|\mathbf{x}_i - \mathbf{x}_j\|) - \frac{\eta}{c} \dot{\mathbf{x}}_i, \quad (7)$$

where E represents the set of edges in the formation graph, and $D_i = |\{j : (i, j) \in E\}|$ is the degree of robot i . This is closely related to the gradient descent update rule over the potential function $\mathcal{E}(x) = \frac{1}{2} \sum_{(i,j) \in E} \mathcal{E}_{ij}(\|\mathbf{x}_i - \mathbf{x}_j\|)$ with an additional damping term, and normalized by the degree of the robot. We will later prove in Section III-C that the degree-normalized potential-based controller and the original potential-based controller have similar behaviors in the sense that the resulting systems converge to the same invariant set.

The main difference between the two distance preserving RMPs is the space that they are defined on. The first RMP is defined on a 1-d distance space while the second RMP is defined on a higher dimensional space. Therefore, the first RMP is more permissive in the sense that the system has more degrees of freedom to achieve other subtasks. This is validated through a formation preservation simulation task in Section V.

C. Potential-based Controllers from RMPs

Designing controllers based-on the gradient descent rule of a potential function is very common in the literature on multi-robot systems, e.g. [16, 9, 10]. Usually, the overall potential function \mathcal{E} is the sum of a set of symmetric, pairwise potential functions $\mathcal{E}_{ij}(\|\mathbf{x}_i - \mathbf{x}_j\|)$ between robot i and robot j that are adjacent in an underlying graph structure. When the robots follow double-integrator dynamics, a damping term is typically introduced to guarantee convergence to an invariant set. Let \mathbf{x} be the ensemble-level state of the team. The controller is given by, $\ddot{\mathbf{x}} = \mathbf{u} = -\nabla \mathcal{E} - \eta \dot{\mathbf{x}}$, where η is a positive scalar. We define a *degree-normalized* potential-based controller as, $\mathbf{u} = \Gamma(\nabla \mathcal{E} - \eta \dot{\mathbf{x}})$, where Γ is a diagonal matrix with $\Gamma_{ii} = 1/D_i$ and D_i is the degree of robot i in the graph.

Theorem III.1. *The degree-normalized version of a potential-based controller converges to the same invariance set as the original potential-based controller.*

Proof: For the original controller, consider the Lyapunov function candidate $V(\mathbf{x}, \dot{\mathbf{x}}) = \frac{1}{2}\|\dot{\mathbf{x}}\|^2 + \mathcal{E}(\mathbf{x})$. Then $\dot{V} = \dot{\mathbf{x}}^\top(\ddot{\mathbf{x}} + \nabla \mathcal{E}) = -\eta \|\dot{\mathbf{x}}\|^2$. By LaSalle's invariance principle [12], the system converges to the invariance set $\{(\mathbf{x}, \dot{\mathbf{x}}) : \nabla \mathcal{E} = 0, \dot{\mathbf{x}} = 0\}$. For the degree-normalized controller, consider the Lyapunov function candidate $V(\mathbf{x}, \dot{\mathbf{x}}) = \frac{1}{2}\dot{\mathbf{x}}^\top \Gamma^{-1} \dot{\mathbf{x}} + \mathcal{E}(\mathbf{x})$. Then $\dot{V} = \dot{\mathbf{x}}^\top(\Gamma^{-1} \dot{\mathbf{x}} + \nabla \mathcal{E}) = -\eta \|\dot{\mathbf{x}}\|^2$. By LaSalle's invariance principle [12], the system also converges to the invariance set $\{(\mathbf{x}, \dot{\mathbf{x}}) : \nabla \mathcal{E} = 0, \dot{\mathbf{x}} = 0\}$ ■

Therefore, similar to the potential-based formation control, one can directly implement the degree-normalized version³ of these potential-based controllers by RMPs defined on the product space, $\mathbf{x} = (\mathbf{x}_i, \mathbf{x}_j)$. The potential function for the RMP is defined as $\Phi(\mathbf{x}) = \mathcal{E}_{ij}(\|\mathbf{x}_i - \mathbf{x}_j\|)$. Constant metric and damping can be used, e.g., $\mathbf{G} \equiv 1$, and $\mathbf{B}(\mathbf{x}, \dot{\mathbf{x}}) = \eta \mathbf{I}$, where η is a positive scalar. Moreover, similar to formation control, one can also define RMPs for these tasks on the distance space $\mathbf{x} = \psi(\mathbf{x}_i, \mathbf{x}_j) = \|\mathbf{x}_i - \mathbf{x}_j\|$ with potential function $\Phi = \mathcal{E}_{ij}$. Since these RMPs are defined on a lower-dimensional manifold, this approach may provide additional degrees of freedom when RMPs are combined with each other.

D. Unitary Goal Attractor

In multi-robot scenarios, instead of planning paths for *every* robot, it is common to plan a path or assign a goal to one robot, called the *leader*. The other robots may simply follow the leader or maintain a given formation depending on other subtasks assigned to the team [17]. In this case, a goal attractor RMP may be assigned to the leader. A number of controllers for multi-robot systems are also based on going to a goal position, such as the cyclic pursuit behavior [9, 15] and Voronoi-based coverage controls [10, 9].

There are several design options for goal attractor RMPs. We will discuss two examples. The first goal attractor RMP

³If the graph is regular, i.e., each robot has the same degree, then the original potential-based controller can be implemented by RMPs.

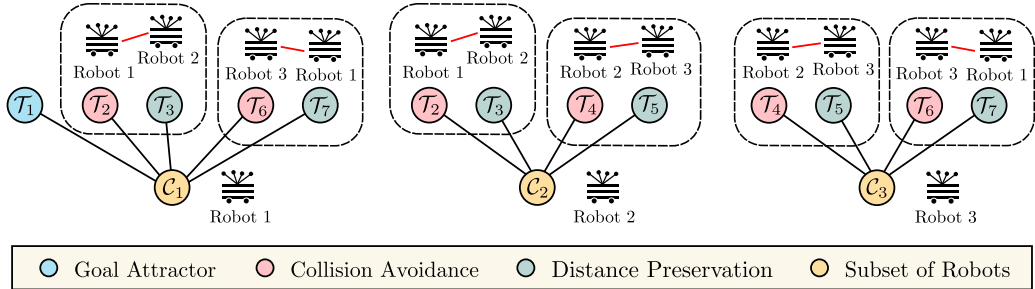


Fig. 2: A decentralized RMP-forest. The three robots are tasked with the same formation preservation task as in Fig. 1. For the decentralized algorithm, each robot has an individual RMP-tree to solve for the control input. All the leaf RMP nodes that are relevant to the robot are attached to its RMP-tree. For example, for robot 1, collision avoidance and distance preservation RMPs for both the pair $\{1, 2\}$ and $\{3, 1\}$ are introduced. There is a goal attractor RMP for robot 1 since it is the leader. Note that there are several copies of the same subtasks in the forest, however, these copies do not share information with each other.

is introduced in [8]. The attractor RMP for robot i is defined on the subtask space $\mathbf{x} = \mathbf{x}_i - \mathbf{g}_i$, where \mathbf{g}_i is the desired configuration for the robot. The metric is designed as $\mathbf{G}(\mathbf{x}) = w(\mathbf{x}) \mathbf{I}$. The weight function $w(\mathbf{x})$ is defined as $w(\mathbf{x}) = \gamma(\mathbf{x}) w_u + (1 - \gamma(\mathbf{x})) w_l$, with $0 \leq w_l \leq w_u < \infty$ and $\gamma(\mathbf{x}) = \exp(-\frac{\|\mathbf{x}\|^2}{2\sigma^2})$ for some $\sigma > 0$. The weights w_l and w_u control the importance of the RMP when the robots are far from the goal and close to the goal, respectively. As the robot approaches the goal, the weight $w(\mathbf{x})$ will smoothly increase from w_l to w_u . The parameter σ determines the characteristic length of the metric. The main intuition for the metric is that when the robot is far from the goal, the attractor should be permissive enough for other subtasks such as collision avoidance, distance preservation, etc. However, when the robot is close to the goal, the attractor should have high importance so that the robot can reach the goal. The gradient of the potential function is designed as,

$$\nabla_{\mathbf{x}} \Phi(\mathbf{x}) = \beta w(\mathbf{x}) \left(\frac{1 - e^{-2\alpha\|\mathbf{x}\|}}{1 + e^{-2\alpha\|\mathbf{x}\|}} \right) \hat{\mathbf{x}} = \beta w(\mathbf{x}) s_\alpha(\|\mathbf{x}\|) \hat{\mathbf{x}}, \quad (8)$$

where $\beta > 0$, $s_\alpha(0) = 0$ and $s_\alpha(r) \rightarrow 1$ as $r \rightarrow \infty$. The parameter α determines the characteristic length of the potential. The potential function defined in (8) provides a *soft-normalization* for \mathbf{x} so that the transition near the origin is smooth. The damping matrix is $\mathbf{B}(\mathbf{x}) = \eta w(\mathbf{x}) \mathbf{I}$, where $\eta > 0$ is a positive scalar. We will refer to this goal attractor RMP as *Goal Attractor RMPa* in subsequent sections. Although more complicated, it produces better results when combined with other RMPs, especially collision avoidance RMPs (see Section V).

Another possible goal attractor RMP is based on a PD controller. This RMP is also defined on the subtask space $\mathbf{x} = \psi(\mathbf{x}_i) = \mathbf{x}_i - \mathbf{g}_i$. The metric is a constant times identity matrix, $\mathbf{G} = c \mathbf{I}$ with some $c > 0$. The potential function is defined as $\Phi(\mathbf{x}) = \frac{1}{2} \alpha \|\mathbf{x}\|^2$ and the damping is $\mathbf{B} = \eta \mathbf{I}$, with $\alpha, \eta > 0$. This RMP is equivalent to a PD controller with $k_p = \alpha/c$ and $k_d = \eta/c$. This goal attractor will be referred to as *Goal Attractor RMPb* in subsequent sections.

IV. DECENTRALIZED CONTROL POLICY GENERATION FOR MULTI-ROBOT SYSTEMS

Although the centralized RMPflow algorithm can be used to generate control policies for multi-robot systems, it can be demanding in both communication and computation. Therefore, we develop a decentralized algorithm that resembles the features of RMPflow while only relying on local communication and computation.

Let \mathcal{L} be the set of all subtasks, and $\{\psi_l\}_{l \in \mathcal{L}}$ be the maps from the configuration space \mathcal{C} to the subtasks spaces $\{\mathcal{T}_l\}_{l \in \mathcal{L}}$. Given the set of all subtasks \mathcal{L} , we say two robots i and j are neighbors if and only if there exists a subtask such that both robots are involved in. Formally,

$$\mathcal{N}_i = \{i \in \mathcal{I} : \{i, j\} \in \mathcal{I}_l \text{ for some } l \in \mathcal{L}\}. \quad (9)$$

We then say that the algorithm is decentralized if only the *state* information of the robot's direct neighbors is required to solve for its control input. Note that here we implicitly assume that the robots are equipped with the sensing modality or communication modality to access the *state* of the neighbors. We also assume that the transformations and the Jacobian matrices for the subtask are known to the robot if it is involved in that subtask. For example, for the formation control task, the robot should know how to calculate distance between two robots given their states, and also know how to take the partial derivatives for the distance function. The major difference between the decentralized algorithms and the centralized RMPflow is that, in the decentralized algorithm, there is no longer a centralized root node that can generate control policies for *all* robots. Instead, each robot should have its *own* tree that generates policies based on the information available locally. Therefore, the decentralized algorithm actually operates on an *forest* with N RMP trees, called the RMP-forest. An example RMP-forest is shown in Fig. 2. Here there are three robots performing the same formation preservation task as in Fig. 1, and hence there are three RMP-trees in the RMP-forest. For each robot, there are leaf RMP nodes for every subtask relevant to the robot. As a result,

there are multiple copies of certain subtasks in the forest, for example, the collision avoidance node for robot 1 and 2 (\mathcal{T}_2) appears twice in the forest: once in the RMP-tree of robot 1, and once in the RMP-tree of robot 2. However, these copies of the same subtask do not share information with each other.

We call the decentralization of RMPflow *partial RMPflow*. As its name suggests, when computing the control input for robot i , the other robots are viewed to be static, i.e., $\dot{\mathbf{q}}_i = 0$. For example, for collision avoidance, each robot would treat all other robots as if they were static obstacles. In this case, every subtask is viewed as a time-varying unitary task. Therefore, following the tree definition in the previous section, it is natural to consider a one-level RMP-tree, where the leaf nodes are directly connected to the root nodes of the trees.

Notationwise, let \mathcal{L}_i be the set of subtasks that robot i participates in. If $l \in \mathcal{L}_i$, let $\psi_{il}(\cdot; \mathbf{q}_{\mathcal{I}_l})$ denote the smooth map from \mathcal{C}_i to the subtask space \mathcal{T}_l , where $\psi_{il}(\mathbf{q}_i; \mathbf{q}_{\mathcal{I}_l}) = \psi_l(\mathbf{q})$. Note that $\psi_{il}(\cdot; \mathbf{q}_{\mathcal{I}_l})$ also depends on the state of other robots $j \in \mathcal{I}_l$. Let \mathbf{J}_{il} be the Jacobian matrix of ψ_{il} with respect to \mathbf{q}_i , i.e., $\mathbf{J}_{il} = \partial_{\mathbf{q}_i} \psi_{il}$.

To compute the control input for robot i , an algorithm similar to RMPflow is applied:

- **pushforward:** Let $\{\mathbf{y}_{il}\}_{l \in \mathcal{L}_i}$ be the coordinates of the leaf nodes of tree i . Given the state of the root, its state is computed as, $\mathbf{y}_{il} = \psi_l(\mathbf{q})$, $\dot{\mathbf{y}}_{il} = \mathbf{J}_{il} \dot{\mathbf{q}}_i$.
- **pullback:** Let $[\mathbf{f}_{il}, \mathbf{M}_{il}]^{\mathcal{T}_l}$ be the RMPs from the leaf l given by the GDS at state $(\mathbf{y}_{il}, \dot{\mathbf{y}}_{il})$. Then we have, $\mathbf{f}_{ri} = \sum_{l \in \mathcal{L}_i} \mathbf{J}_{il}^\top (\mathbf{f}_{il} - \mathbf{M}_{il} \dot{\mathbf{J}}_{il} \dot{\mathbf{q}}_i)$, $\mathbf{M}_{ri} = \sum_{l \in \mathcal{L}_i} \mathbf{J}_{il}^\top \mathbf{M}_{il} \mathbf{J}_{il}$.
- **resolve:** The control input is given by $\mathbf{u}_{ri} = \mathbf{M}_{ri}^\dagger \mathbf{f}_{ri}$.

Note that when all the metrics are constant diagonal matrices and all the Jacobian matrices are identity matrices, the decentralized RMP framework has exactly the same behavior as RMPflow. This, in particular, holds for the degree-normalized potential-based controllers discussed in III-C. Therefore, the decentralized RMP framework can also reconstruct a large number of multi-robot controllers up to degree normalization.

Partial RMPflow has a stability result similar to RMPflow, which is stated in the following theorem.

Theorem IV.1. *Let \mathbf{G}_{ri} , \mathbf{B}_{ri} and Φ_{ri} be the metric, damping matrix, and potential of the tree i 's root node. If $\mathbf{G}_{ri}, \mathbf{B}_{ri} \succ 0$ for all $i \in \mathcal{I}$, the system converges to a forward invariant set $\mathcal{C}_\infty := \{(\mathbf{q}, \dot{\mathbf{q}}) : \nabla_{\mathbf{q}_i} \Phi_{ri} = 0, \dot{\mathbf{q}}_i = 0, \forall i \in \mathcal{I}\}$.*

Proof: Let Φ be the total potential function for all subtasks, i.e., $\Phi = \sum_{l \in \mathcal{L}} \Phi_l \circ \psi_l$. Consider the Lyapunov function candidate $V = \sum_{i=1}^N K_i + \Phi$, where, $K_i = \frac{1}{2} \dot{\mathbf{q}}_i^\top \mathbf{G}_{ri} \dot{\mathbf{q}}_i$. By [8],

$$\begin{aligned} \frac{d}{dt} K_i &= \frac{d}{dt} \left(\frac{1}{2} \dot{\mathbf{q}}_i^\top \left(\sum_{l \in \mathcal{L}_i} \mathbf{J}_{il}^\top \mathbf{G}_{il} \mathbf{J}_{il} \right) \dot{\mathbf{q}}_i \right) \\ &= \dot{\mathbf{q}}_i^\top \sum_{l \in \mathcal{L}_i} \mathbf{J}_{il}^\top (-\nabla_{\mathbf{y}_{il}} \Phi_l - \mathbf{B}_l \mathbf{J}_{il}^\top \dot{\mathbf{q}}_i) \\ &= -\dot{\mathbf{q}}_i^\top \mathbf{B}_{ri} \dot{\mathbf{q}}_i - \sum_{l \in \mathcal{L}_i} \dot{\mathbf{y}}_{il}^\top \nabla_{\mathbf{y}_{il}} \Phi_l \end{aligned} \quad (10)$$

Hence, we have,

$$\begin{aligned} \frac{d}{dt} V &= \sum_{i=1}^N \frac{d}{dt} K_i + \sum_{l \in \mathcal{L}} \dot{\mathbf{y}}_l^\top \nabla_{\mathbf{y}_l} \Phi_l \\ &= \sum_{l \in \mathcal{L}} \left(- \left(\sum_{i \in \mathcal{I}_l} \dot{\mathbf{y}}_{il}^\top \right) + \dot{\mathbf{y}}_l^\top \right) \nabla_{\mathbf{y}_l} \Phi_l \\ &\quad - \sum_{i=1}^N \dot{\mathbf{q}}_i^\top \mathbf{B}_{ri} \dot{\mathbf{q}}_i \\ &= - \sum_{i=1}^N \dot{\mathbf{q}}_i^\top \mathbf{B}_{ri} \dot{\mathbf{q}}_i, \end{aligned} \quad (11)$$

where the second equation follows from the fact that $\mathbf{y}_{il} = \psi_{il}(\mathbf{q}_i; \mathbf{q}_{\mathcal{I}_l}) = \psi_l(\mathbf{q}) = \mathbf{y}_l$ for all $i \in \mathcal{I}_l$, and the third follows from $\dot{\mathbf{y}}_l = \sum_{i \in \mathcal{I}_l} \mathbf{J}_{il} \dot{\mathbf{q}}_i = \sum_{i \in \mathcal{I}_l} \dot{\mathbf{y}}_{il}$. Then by LaSalle's invariance principle [12] and Theorem 1 in [8], the system converges to a forward invariant set $\mathcal{C}_\infty := \{(\mathbf{q}, \dot{\mathbf{q}}) : \nabla_{\mathbf{q}_i} \Phi_{ri} = 0, \dot{\mathbf{q}}_i = 0, \forall i \in \mathcal{I}\}$. ■

V. EXPERIMENTAL RESULTS

We evaluate the multi-robot RMP framework through both simulation and robotic implementation. In simulation, we focus on comparing RMPs with existing multi-robot controllers and also comparing different design choices of RMPs with each other. In the second part of this section, two experiments illustrate the performance of centralized and decentralized multi-robot RMPs, respectively.

A. Simulation Results

1) **RMPs & Potential-based Controllers:** As is discussed in Section III, many potential-based multi-robot controllers can be reconstructed by the RMP framework up to degree normalization. In this example, we consider a formation control task with five robots. The robots are tasked with forming a regular pentagon with circumcircle radius 0.4. The robots are initialized with a regular pentagon formation, but with a larger circumcircle radius of 1. We consider a degree-normalized potential field controller from [16],

$$\begin{aligned} \mathbf{u}_i &= -\frac{1}{D_i} \sum_{j:(i,j) \in E} \left(\partial_{x_i} \left\{ \frac{1}{2} (\|\mathbf{x}_i - \mathbf{x}_j\| - d_{ij})^2 \right\} - \eta \dot{\mathbf{x}}_i \right) \\ &= -\frac{1}{D_i} \sum_{j:(i,j) \in E} \left(\frac{\|\mathbf{x}_i - \mathbf{x}_j\| - d_{ij}}{\|\mathbf{x}_i - \mathbf{x}_j\|} (\mathbf{x}_i - \mathbf{x}_j) - \eta \dot{\mathbf{x}}_i \right), \end{aligned} \quad (12)$$

where d_{ij} is the desired distance between robot i and robot j , E is the set of edges in the formation graph, and D_i is the degree of robot i in the formation graph. For the RMP implementation, we use the controller given by (7). The potential-based controller (12) is equivalent to the controller generated by the distance preservation RMP given by (7) when choosing $c = \alpha = 1$. In simulation, we choose $\eta = 2$ for both the RMP controller and the potential-based controller. The trajectories of the robots under the two controllers are displayed in Fig. 3a and Fig. 3b, respectively. The results are *identical* implying the controllers have exactly the same behavior.

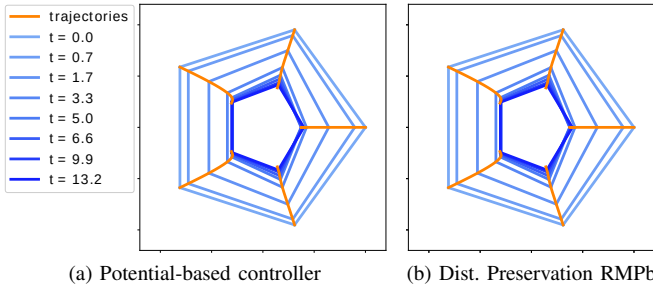


Fig. 3: (a) The potential-based controller introduced in [16]. The blue pentagons from light to dark denotes the shape from $t = 0.0s$ to $t = 13.2s$. The orange curves represent the trajectories of the robots. (b) The controller generated from the centralized RMP framework with Distance Preservation RMPa. The fact that (a) and (b) are identical shows that the two controllers have exactly the same behavior.

2) Distance Preservation RMPs & Formation Preservation:

One of the main features of the RMP framework is that controllers are defined on their corresponding task manifolds rather than the configuration space. This provides a natural mechanism to combine controllers for different objectives. For example, formation preservation tasks [2, 3], where robots must maintain a certain formation while the leader is driven by some external force, are considered harder than formation control tasks since one needs to carefully balance the external force and the formation controller. However, since translations and rotations can still preserve shape, the team *should* have the capability of maintaining the formation regardless of the motion of the leader.

We consider a formation preservation task in simulation where a team of five robot are tasked with forming a regular pentagon while the leader has an additional task of reaching a goal located at $(1, 1)$. The two distance preservation RMPs introduced in Section III-B are compared. Distance preservation RMPs are defined for all edges in the formation graph and an additional goal attractor RMPa is defined for one of the robots, with parameters $w_u = 10$, $w_l = 1$, $\sigma = 0.1$, $\alpha = \eta = 1$. We use a damper RMP defined by a GDS on the configuration space of every single robot with $\mathbf{G} \equiv 0.01 \mathbf{I}$ $\mathbf{B} \equiv \mathbf{I}$, $\Phi \equiv 0$ so that they can reach a full stop at the goal. Fig. 4a shows the resulting behavior for the distance preserving RMPa, with parameters $\mathbf{G} = c = 1$ and $\eta = 2$. The robots manage to preserve shape while the leader robot is reaching the goal since the subtasks are defined on lower dimensional manifolds. By contrast, the behavior for distance preservation RMPb (which is shown to be equivalent to the potential-based controller in the previous simulation), with parameters $\mathbf{G} = \mathbf{I}$ and $\eta = 2$ is shown in Fig. 4b. This distance preservation RMP fails to maintain the formation when the leader robot is attracted to the goal.

3) Goal Attractor RMPs & Collision Avoidance RMPs: An advantage of the multi-robot RMP framework is that it can leverage existing single-robot controllers, which may have

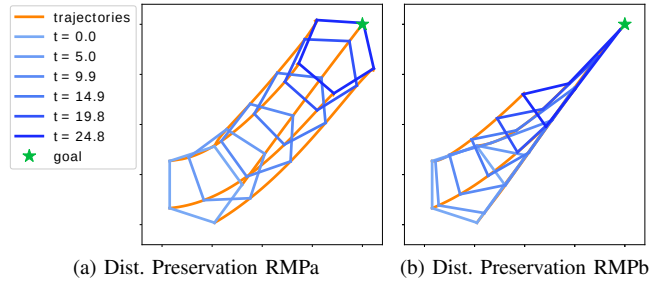


Fig. 4: (a) The behavior of distance preservation RMPa when combined with a goal attractor RMP. The blue pentagons from light to dark denotes the shape from $t = 0.0s$ to $t = 24.8s$. The orange curves show the trajectories of the robots. The robots manage to reach the goal while maintaining the shape. (b) The same experiment with distance preservation RMPb. The robots fail to maintain the shape.

desirable properties, especially when combined with other controllers. In this simulation task, the performance of the two goal attractor RMPs are compared when combined with pairwise collision avoidance RMPs. In the simulation, three robots are tasked with reaching a goal on the other side of the field while avoiding collisions with each of the others. The parameters for the collision avoidance RMPs are set as $\alpha = \epsilon = 1e-5$, and $\eta = 0.2$. Fig. 5a and Fig. 5b show the behavior of the resulting controllers with the two choices goal attractor RMPs discussed in Section III-D, respectively. For goal attractor RMPa, we use parameters $w_u = 10$, $w_l = 0.01$, $\sigma = 0.1$, $\alpha = 1$, and $\eta = 1$. we use $c = 1$, $\alpha = 1$, and $\eta = 2$ for goal attractor RMPb. We notice that goal attractor RMPa generates smoother trajectories compared to goal attractor RMPb.

4) The Centralized & Decentralized RMP Algorithms: The centralized and the decentralized RMP algorithms are also compared through the same simulation of three robots reaching goals. Goal attractor RMPa's with the same parameters were used. For the collision avoidance RMP, we set $\alpha = \epsilon = 1e-5$, and $\eta = 0.2$. The trajectories of the robots under the decentralized algorithm are illustrated in Fig. 5c. Compared to trajectories generated from centralized RMPs, the robots oscillate slightly when approaching other robots, and made aggressive turns to avoid collisions.

B. Robotic Implementations

We present several experiments (video: <https://youtu.be/VZHR5SN9wXk>) conducted on the Robotarium [18], a remotely accessible swarm robotics platform. Since the centralized and decentralized multi-robot RMP frameworks have their own individual features, we design a separate experiment for each framework to show their full capability.

1) Centralized Multi-Robot RMPs: The main advantage of the centralized multi-robot framework is that the subtask spaces are jointly considered and hence the behavior of each controller is combined consistently. To fully exploit this fea-

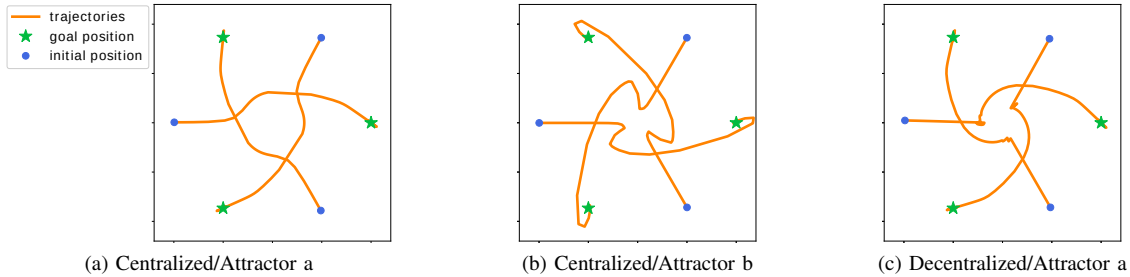


Fig. 5: The performance of goal attractor RMPs combined with pairwise collision avoidance RMPs. The blue dots and red stars denote the initial and goal positions, respectively. The trajectories are represented by orange curves. (a) The more sophisticated goal attractor RMPa generates smooth trajectories when combined with collision avoidance RMP in the centralized framework. (b) Goal attractor RMPb, which is equivalent to a PD controller, generates more distorted trajectories. (c) Under the decentralized RMP framework, the robots oscillate slightly near the origin and turn abruptly against each other.

ture, we consider formation preservation with two sub-teams of robots. The two sub-teams are tasked with maintaining their formation while moving back and forth between two goal points A and B . The five robots in the first sub-team are assigned a regular pentagon formation and the four robots in the second sub-team must form a square. At the beginning of the task, goal A is assigned to the first sub-team and goal B to the second sub-team. When both sub-teams arrive at their corresponding goals, the goal position is swapped so that the robots can move back and forth between the goals. The robots are expected to negotiate their path so that their trajectories are collision free.

A combination of distance preservation RMPs, collision avoidance RMPs, goal attractor RMPs, and damper RMPs are used to achieve this behavior. The construction of the RMP-tree is similar to Fig. 1. A distance preservation RMPa with $\mathbf{G} = \mathbf{c} = 10$, and $\eta = 5$ is assigned to every pair of robots that corresponds to an edge in the formation graph, while collision avoidance RMPs are defined for every pair of robots. The safety distance between robots is $R_s = 0.18$. The parameters for the collision avoidance RMPs are set as $\alpha = 1e - 5$, $\epsilon = 1e - 8$, and $\eta = 0.5$. For each sub-team, we define a goal attractor RMPa for the leader. For goal attractor RMPa's, we set $w_u = 10$, $w_l = 0.01$, $\sigma = 0.1$, $\beta = 1$, $\alpha = 1$, and $\eta = 1$. We also use a damper RMP defined by a GDS on the configuration space of every single robot with $\mathbf{G} \equiv 0.01 \mathbf{I}$, $\mathbf{B} \equiv \mathbf{I}$, $\Phi \equiv 0$ so that the robots can reach a full stop at the goal. Fig. 6 shows several snapshots from the experiment. We see that the robots are able to maintain their corresponding formations while avoiding collision. An interesting observation is that the two sub-teams of robots rotated around each other to avoid potential collision, which shows that the full degrees of freedom of the formation preservation task was exploited.

2) *Decentralized Multi-Robot RMPs*: For the decentralized multi-robot RMP framework, we consider a team of eight robots. The robots are divided into two sub-teams. The task of the first sub-team is to achieve cyclic pursuit behavior for a circle of radius 1 m centered at the origin. The other sub-team is designed to go through the circle surveilled by the other sub-team. The RMP-forest for the second sub-team

follows a similar structure as Fig. 2. For the cyclic pursuit tasks, the robots are attracted by points moving along the circle with angular velocity 0.06 rad/s. The goal attractors are goal attractor RMPb's with parameters with $G = c = 5\mathbf{I}$, $\alpha = 1$, and $\eta = 2$. For robots from sub-team 2, the distance preservation RMPa's have parameters $\mathbf{G} = \mathbf{c} = 10$, $\eta = 2$. The goal attractor for the leader in sub-team 2 is a goal attractor RMPa, with parameters $w_u = 10$, $w_l = 1$, $\sigma = 0.1$, $\beta = 0.1$, $\alpha = 10$, $\eta = 2$. For each single robot, there are decentralized collision avoidance RMPs for all other robots. The parameters for the collision avoidance RMPs are $\alpha = 1e - 5$, $\epsilon = 1e - 8$, and $\eta = 1$, with safety distance $R_s = 0.18$. Snapshots from the experiment are shown in Fig. 7. The robots from the second sub-team manage to pass through the circle under the decentralized multi-robot RMP framework.

C. Discussion

A significant feature of RMPs is that they are intrinsically coordinate-free [8]. Consider two robots i and j with configuration space \mathcal{C}_i and \mathcal{C}_j , respectively. Assume that there exists a smooth mapping ψ from \mathcal{C}_j to \mathcal{C}_i . Then the RMP-tree designed for one robot i can be directly transferred to robot j by connecting the tree to the root node of robot j through the mapping ψ . Therefore, RMPs provide a level of abstraction for heterogeneous robotic teams so that the user only needs to design desired behaviors for a homogeneous team with simple dynamics models, for example, double integrator dynamics, and seamlessly transfer it to the heterogeneous team. This insight could bridge the gap between theoretical results, which are usually derived for homogeneous robotic teams with simple dynamics models, and real robotics applications.

VI. CONCLUSIONS

In this paper, we consider multi-objective tasks for multi-robot systems. We argue that it is advantageous to define controllers for single subtasks on their corresponding manifolds. We propose centralized and decentralized algorithms to generate control policies for multi-robot systems by combining control policies defined for individual subtasks. The multi-robot system is proved to be stable under the control policies generated by the proposed algorithms. We show that many

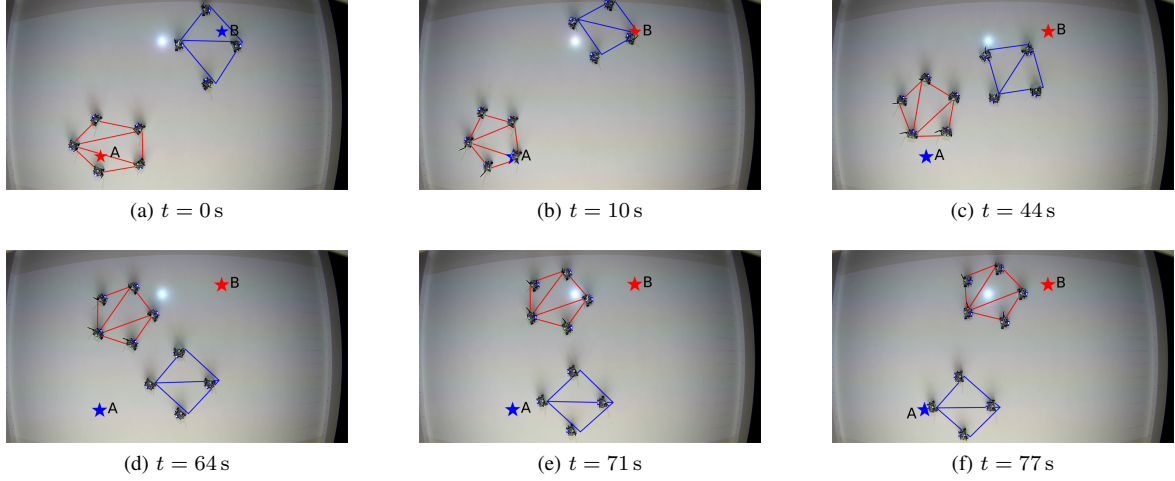


Fig. 6: The snapshots from the formation preservation experiment with the centralized multi-robot RMP framework. Goal positions and the formation graphs are projected onto the arena by an overhead projector. The colors of the graphics are augmented in the figures for the purpose of visualization. The two sub-teams of robots are tasked with maintaining the formation while moving back and forth between two goal points in arena. The red and blue lines in the figure denote the formation graphs. The red and blue stars are the current goal positions for sub-team 1 and sub-team 2, respectively.

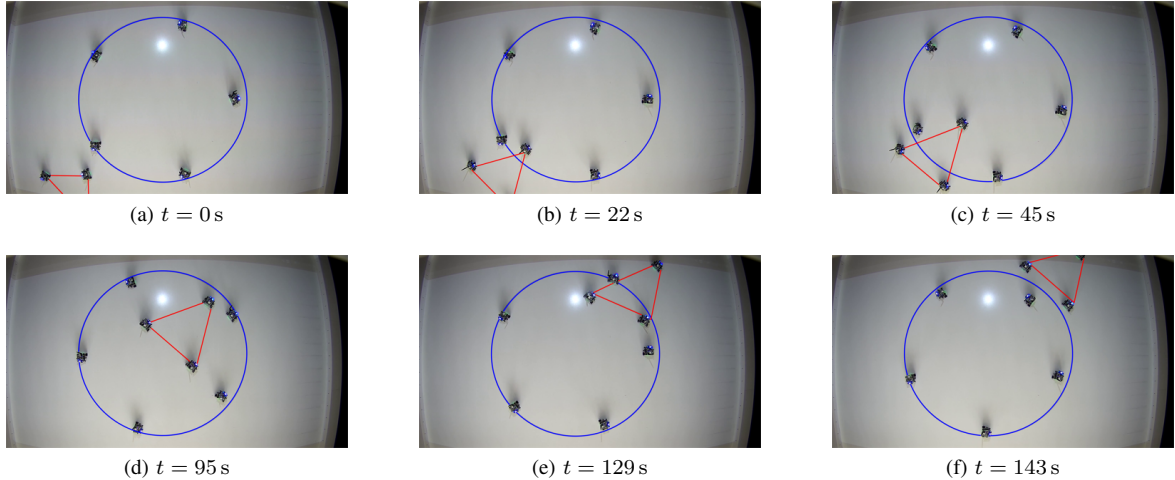


Fig. 7: The snapshots from the experiment for the decentralized multi-robot RMP framework. The circle surveilled by the first sub-team and the formation graph for the second sub-team are projected onto the environment. Robots were divided into two sub-teams. The first sub-team of five robots performed a cyclic pursuit behavior for a circle of radius 1 centered at the origin. The other sub-team of three robots passed through the circle surveilled by the other sub-team without collisions.

existing potential-based multi-robot controllers can also be approximated by the proposed algorithms. Several subtask policies are proposed for multi-robot systems and tested through numerical simulation and deployment on real robots.

REFERENCES

- [1] Aaron D Ames, Jessy W Grizzle, and Paulo Tabuada. Control barrier function based quadratic programs with application to adaptive cruise control. In *Decision and Control (CDC), 2014 IEEE 53rd Annual Conference on*, pages 6271–6278. IEEE, 2014.
- [2] Brian DO Anderson, Changbin Yu, Baris Fidan, and Julien M Hendrickx. Rigid graph control architectures for autonomous formations. *IEEE Control Systems Magazine*, 28(6):48–63, 2008.
- [3] Gianluca Antonelli, Filippo Arrichiello, and Stefano Chiaverini. Flocking for multi-robot systems via the null-space-based behavioral control. *Swarm Intelligence*, 4(1):37, 2010.
- [4] Ronald C Arkin, Ronald C Arkin, et al. *Behavior-based robotics*. MIT press, 1998.
- [5] Urs Borrman, Li Wang, Aaron D Ames, and Magnus B

Egerstedt. Control barrier certificates for safe swarm behavior. Georgia Institute of Technology, 2015.

[6] Francesco Bullo and Andrew D Lewis. *Geometric control of mechanical systems: modeling, analysis, and design for simple mechanical control systems*, volume 49. Springer Science & Business Media, 2004.

[7] Francesco Bullo, Jorge Cortes, and Sonia Martinez. *Distributed control of robotic networks: a mathematical approach to motion coordination algorithms*, volume 27. Princeton University Press, 2009.

[8] Ching-An Cheng, Mustafa Mukadam, Jan Issac, Stan Birchfield, Dieter Fox, Byron Boots, and Nathan Ratliff. Rmpflow: A computational graph for automatic motion policy generation. *arXiv preprint arXiv:1811.07049*, 2018.

[9] Jorge Cortés and Magnus Egerstedt. Coordinated control of multi-robot systems: A survey. *SICE Journal of Control, Measurement, and System Integration*, 10(6):495–503, 2017.

[10] Jorge Cortes, Sonia Martinez, Timur Karatas, and Francesco Bullo. Coverage control for mobile sensing networks. *IEEE Transactions on robotics and Automation*, 20(2):243–255, 2004.

[11] Vishnu R Desaraju and Jonathan P How. Decentralized path planning for multi-agent teams with complex constraints. *Autonomous Robots*, 32(4):385–403, 2012.

[12] Hassan K Khalil. Nonlinear systems. *Prentice-Hall, New Jersey*, 2(5):5–1, 1996.

[13] O. Khatib. Real-time obstacle avoidance for manipulators and mobile robots. In *IEEE International Conference on Robotics and Automation (ICRA)*, volume 2, pages 500–505, Mar 1985. doi: 10.1109/ROBOT.1985.1087247.

[14] Wenhao Luo, Nilanjan Chakraborty, and Katia Sycara. Distributed dynamic priority assignment and motion planning for multiple mobile robots with kinodynamic constraints. In *American Control Conference (ACC)*, 2016, pages 148–154. IEEE, 2016.

[15] Joshua A Marshall, Mireille E Broucke, and Bruce A Francis. Formations of vehicles in cyclic pursuit. *IEEE Transactions on automatic control*, 49(11):1963–1974, 2004.

[16] Mehran Mesbahi and Magnus Egerstedt. *Graph theoretic methods in multiagent networks*, volume 33. Princeton University Press, 2010.

[17] Reza Olfati-Saber. Flocking for multi-agent dynamic systems: Algorithms and theory. *IEEE Transactions on automatic control*, 51(3):401–420, 2006.

[18] Daniel Pickem, Paul Glotfelter, Li Wang, Mark Mote, Aaron Ames, Eric Feron, and Magnus Egerstedt. The robotarium: A remotely accessible swarm robotics research testbed. In *Robotics and Automation (ICRA), 2017 IEEE International Conference on*, pages 1699–1706. IEEE, 2017.

[19] Nathan D Ratliff, Jan Issac, Daniel Kappler, Stan Birchfield, and Dieter Fox. Riemannian motion policies. *arXiv preprint arXiv:1801.02854*, 2018.

[20] Siddharth Swaminathan, Mike Phillips, and Maxim Likhachev. Planning for multi-agent teams with leader switching. In *Robotics and Automation (ICRA), 2015 IEEE International Conference on*, pages 5403–5410. IEEE, 2015.

[21] Glenn Wagner and Howie Choset. Subdimensional expansion for multirobot path planning. *Artificial Intelligence*, 219:1–24, 2015.

[22] Li Wang, Aaron D Ames, and Magnus Egerstedt. Multi-objective compositions for collision-free connectivity maintenance in teams of mobile robots. In *Decision and Control (CDC), 2016 IEEE 55th Conference on*, pages 2659–2664. IEEE, 2016.